Editors' Suggestion Featured in Physics

Production of p Nuclei from r-Process Seeds: The νr Process

Zewei Xiong,[1,*] Gabriel Martínez-Pinedo,[1,2,3] Oliver Just,[1,4] and Andre Sieverding[5]

[1]*GSI Helmholtzzentrum für Schwerionenforschung, Planckstraße 1, D-64291 Darmstadt, Germany*
[2]*Institut für Kernphysik (Theoriezentrum), Fachbereich Physik, Technische Universität Darmstadt, Schlossgartenstraße 2, D-64289 Darmstadt, Germany*
[3]*Helmholtz Forschungsakademie Hessen für FAIR, GSI Helmholtzzentrum für Schwerionenforschung, Planckstraße 1, 64291 Darmstadt, Germany*
[4]*Astrophysical Big Bang Laboratory, RIKEN Cluster for Pioneering Research, 2-1 Hirosawa, Wako, Saitama 351-0198, Japan*
[5]*Max Planck Institute for Astrophysics, Karl-Schwarzschild-Straße 1, D-85748 Garching, Germany*

(Received 18 May 2023; revised 29 December 2023; accepted 13 March 2024; published 9 May 2024)

We present a *new* nucleosynthesis process that may take place on neutron-rich ejecta experiencing an intensive neutrino flux. The nucleosynthesis proceeds similarly to the standard r process, a sequence of neutron captures and beta decays with, however, charged-current neutrino absorption reactions on nuclei operating much faster than beta decays. Once neutron-capture reactions freeze out the produced r process, neutron-rich nuclei undergo a fast conversion of neutrons into protons and are pushed even beyond the β stability line, producing the neutron-deficient p nuclei. This scenario, which we denote as the νr process, provides an alternative channel for the production of p nuclei and the short-lived nucleus ^{92}Nb. We discuss the necessary conditions posed on the astrophysical site for the νr process to be realized in nature. While these conditions are not fulfilled by current neutrino-hydrodynamic models of r-process sites, future models, including more complex physics and a larger variety of outflow conditions, may achieve the necessary conditions in some regions of the ejecta.

DOI: 10.1103/PhysRevLett.132.192701

Introduction.—A variety of processes have been suggested as the origin of stable nuclei heavier than iron and located at the neutron-deficient side of the β-stability line, the so-called p nuclei. Those include the γ process (p process) [1,2], νp process [3–5], and rp process [6].

In the γ process, seed nuclei present from the initial composition of the star, undergo (γ, n) reactions followed by (γ, p) or (γ, α) as the temperature rises to 3–5 GK in core-collapse and Type Ia supernovae [2,7–9]. While its yields are consistent for more than half of the p nuclei, some specific regions, such as ^{92,94}Mo and ^{96,98}Ru, are underproduced. The γ process is not a primary process and depends on the preexisting s-process seeds.

On the other hand, p nuclei can also be produced in the νp process through proton capture aided by neutrinos in neutrino-driven winds from core-collapse supernovae (CCSNe) [3,10]. Long β^+ decay times of waiting-point nuclei such as ^{64}Ge can be circumvented by (n, p) reactions with neutrons produced by absorption of electron antineutrinos on protons. However, current three-dimensional supernova models suggest that a neutrino-driven wind may not develop except for low mass progenitors [11]. Furthermore, neutrino-wind simulations based on up-to-date set of neutrino opacities produce ejecta not proton-rich enough for a strong νp process [12].

Light p nuclei, like ^{92}Mo, may also be produced in the inner ejecta of CCSN by explosive nucleosynthesis [13–15], but no substantial production occurs of heavier ones. Light p nuclei can also be produced by the rp process in accreting neutron stars [6], but it is an open question whether and how material is ejected from the neutron star and contributes to galactic chemical evolution.

In addition to p nuclei, another element of yet unknown origin is the by now extinct nucleus ^{92}Nb that existed in the early solar system (ESS) [16–19]. It cannot be produced by the νp or rp processes as it is shielded by ^{92}Mo [20]. The production of ^{92}Nb through the γ process is viable but the yield falls short of explaining the amount measured in the ESS, probably related to the underproduction of ^{92,94}Mo and ^{96,98}Ru [21]. A feasible way of production could be through charge-current (CC) and neutral-current (NC) weak interactions on the preexisting nuclei ^{92}Zr and ^{93}Nb in the ν process [18,22,23].

Previous studies of the r process both in the context of CCSNe and binary neutron star mergers (BNM) have shown that neutrinos play a fundamental role. At high temperatures, when the composition consists of neutrons and protons, electron (anti)neutrino absorption and the inverse reactions determine the neutron richness of the ejected material [24–28]. This aspect is fundamental to produce ejecta with a broad distribution of neutron richness and to account for the observation of Sr in the AT2017gfo kilonova [29]. Large neutrino fluxes are in general detrimental for the *r* process as they drive the composition to proton-to-nucleon ratios of $Y_e \approx 0.5$ due to the operation of the α effect [30,31]. Once nuclei form, substantial neutrino fluxes hinder the *r* process by converting neutrons into protons and reducing the amount of neutrons available for captures. Furthermore, large rates of electron neutrino absorption on nuclei hinder the formation of *r*-process peaks associated to magic numbers [32–34].

This regime of large neutrino fluxes, when electron-neutrino absorption rates are faster than beta decays for neutron-rich nuclei, is precisely the regime we consider in this Letter. We will show that it leads to a *new* nucleosynthesis process that produces *p* nuclei and ^{92}Nb operating on seeds produced by the *r* process under strong irradiation by neutrinos. We denote this process as νr process. Unlike γ, νp, or rp processes that occur in proton-rich conditions, the νr process operates in neutron-rich conditions. The large neutrino fluxes restrict the conditions at which it operates to $Y_e \approx 0.4$–0.5. It requires several stages for the production of *p* nuclei. The nucleosynthesis starts at high temperatures with a composition of neutrons and protons. As the temperature decreases, nuclei are formed by charged-particle reactions that freeze out at temperatures $T \sim 3$ GK. This phase results in an α-rich composition characteristic of the operation of the α process [35,36]. The produced nuclei act as seeds for further neutron captures along a path determined by $(n,\gamma)\rightleftarrows(\gamma,n)$ equilibrium. In the absence of neutrino irradiation, the equilibrium is broken by beta decays that determine the speed at which heavy elements are built and the rate at which neutrons are exhausted. When this happens, neutron captures freeze out and nuclei undergo beta decay and migrate toward the valley of stability.

This picture, however, is drastically changed if the ejecta are irradiated by a large neutrino flux. Large neutrino-absorption rates dominate the flow to higher charge numbers instead of beta decays, leading to faster depletion of neutrons. This speeds up the production of heavy elements and leads to an earlier freeze-out of neutron captures at higher temperatures compared with the case without neutrino fluxes. Unlike the *r* process, in which after the freeze-out material moves to the stability by beta decays stopping at the first stable nucleus, in the νr process CC neutrino-nucleus reactions drive the matter to and beyond the stability line. Furthermore, the energy of neutrinos is larger than the neutron, proton, and alpha separation energies, and hence CC and NC neutrino-nucleus reactions produce free neutrons, protons, and α particles that are captured at the still relatively high temperatures. This leads to a broader abundance distribution that reaches from neutron-deficient to neutron-rich nuclei on both sides of the stability line and the production of significant amounts of *p* nuclei.

Parametric trajectory.—We use the nuclear reaction network (employed previously in, e.g., Refs. [37,38]) with the reaction rates based on the finite-range droplet mass model [39] and a consistent description of neutrino reactions with nucleons (ν-N) and nuclei (ν-A) that considers light particle spallation induced by both NC and CC ν-A reactions [22]. We neglect finite temperature corrections to the neutrino-nucleus cross sections.

We assume adiabatic expansions starting with an initial temperature of $T_0 = 10$ GK and density of $\rho_0 = 4.6 \times 10^6\ \mathrm{g\,cm^{-3}}$ that corresponds to an initial entropy per nucleon, $s = 84\ k_B$. We assume homologous expansion for the density evolution $\rho(t) = \rho_0(1 + t/\delta_\rho)^{-3}$. The temperature is evolved accounting for the energy generation by nuclear reactions [40]. δ_ρ is related to the expansion timescale $\tau_{\mathrm{exp}} = -[d \ln \rho(t)/dt]^{-1} = (t + \delta_\rho)/3$. We fix the initial electron fraction, $Y_{e,0}$, that is subsequently evolved under the influence of (anti)neutrino absorption and their inverse reactions. Neutrino number densities are parametrized as $n_{\nu_e}(t) = n_{\nu_e,0}(1 + t/\delta_\nu)^{-3}$ and $n_{\bar{\nu}_e}(t) = R_n n_{\nu_e}(t)$, where $\delta_\nu \geq \delta_\rho$ (because the neutrino flux may decrease more slowly than the baryon density at small radii, e.g., due to polar focusing of radiation in an accretion disk [41]), and R_n is a constant ratio relating the $\bar{\nu}_e$ and ν_e densities. The power index -3 accounts for both inverse-square radial dependence of the neutrino flux at $t \gtrsim \delta_\nu$ and the decay of the neutrino luminosity assumed here $\propto t^{-1}$. Neutrino spectra are approximated by Fermi-Dirac distributions with constant effective temperatures T_{ν_e} and $T_{\bar{\nu}_e}$.

Figure 1 compares the abundances from three trajectories I–III with parameters $[\delta_\rho(\mathrm{ms}), n_{\nu_e,0}(10^{32}\ \mathrm{cm^{-3}})]$ of [4,2.5], [1, 10], and [0.5, 20], respectively. The other parameters have the values $Y_{e,0} = 0.4$, $R_n = 1.2$, $\delta_\nu = 4\delta_\rho$, $T_{\nu_e} = 5$ MeV, and $T_{\bar{\nu}_e} = 1.25 T_{\nu_e}$. We find that Y_e reaches ≈ 0.467 at $T = 5$ GK in all three cases. At this temperature, the rapid expansion of moderately neutron-rich matter gives high neutron-to-seed ratios n_s (13.8, 59.2, and 177, respectively), and allows an *r* process to occur.

Abundances.—Without ν-A reactions, case I corresponds to the α-rich freeze-out with moderate neutron-rich conditions, such as considered in Refs. [5,13,43], that is known to produce ^{92}Mo but not ^{94}Mo. Once the ν-A reactions are included, the ratio ^{92}Mo/^{94}Mo becomes consistent with solar proportions and the yield of the radioactive ^{92}Nb is also enhanced. Despite their much larger n_s at 5 GK that would usually allow for a much stronger *r* process, the abundance peaks for cases II and III only moderately shift to higher mass numbers when compared to case I. The larger neutrino densities lead to a conversion of neutrons

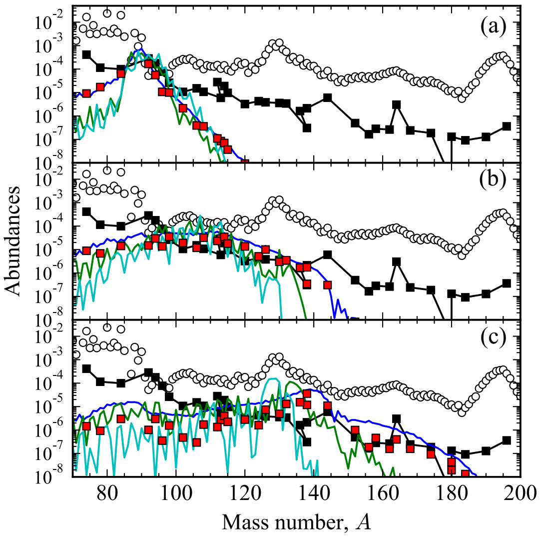

FIG. 1. Comparison of the isobaric yields at 1 Gyr (blue curves) and the abundance of p nuclei on those yields (red squares) with the solar abundances of p nuclei (black squares) [1] and r nuclei (black circles) [42] in cases I (a), II (b), and III (c). Green and cyan curves show the yields at $n_s \sim 1$ with and without ν-A reactions, respectively.

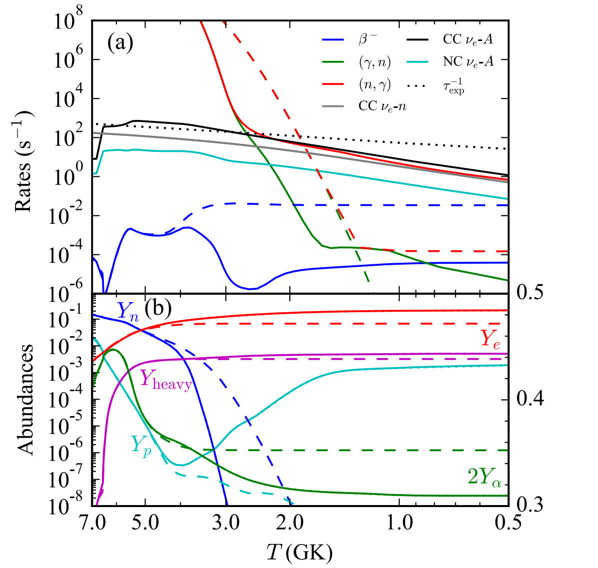

FIG. 2. Average rates (a) and abundances (b) as functions of temperature including (solid) and neglecting (dashed) ν-A reactions in case I. Y_α and Y_e are shown with the scale labeled on the right side.

into protons while the r process operates and reduces the amount of neutrons for captures on heavy nuclei. When $n_s \sim 1$ is reached, the initial supply of neutrons is almost depleted. Figure 1 compares the abundances at this time with and without ν-A interactions (cyan vs green lines), illustrating that ν-A interactions speed up the flow to heavier isotopes. The difference between the abundances at $n_s \sim 1$ and the final abundances shows the impact of the additional neutrons produced by the neutrino spallation reactions.

All those three cases show comparable amounts of p nuclei produced relative to the final total yield at mass numbers close to the respective abundance peak, which indicates a successful conversion of those r-process seeds. The abundance pattern in case I shows a peak around ^{92,94}Mo and ^{96,98}Ru. Larger n_s in cases II and III lead to the production of p nuclei up to $A \sim 145$ and 180, respectively. Heavier p nuclei up to ^{196}Hg can be produced with higher neutrino number densities.

Reaction dynamics.—We compare the averaged rates for β^- decay, (n,γ), (γ,n), CC, and NC ν_e-A reactions for case I in Fig. 2(a). They are computed as $\lambda_I = \sum_i \lambda_{I,i} Y_i / Y_{\rm heavy}$, where I stands for a particular reaction, i sums over all heavy nuclei ($A > 4$), and $Y_{\rm heavy} = \sum_i Y_i$ is the total abundance of heavy nuclei. The ν_e-n rate $\lambda_{\nu_e n} = n_{\nu_e} \sigma_{\nu_e n} c$ is approximately 1 ms^{-1} for $n_{\nu_e} = 10^{33}$ cm^{-3} and $T_{\nu_e} = 5$ MeV. The CC rates $\lambda^{\rm CC}_{\nu_e A,i} = n_{\nu_e} \sigma^{\rm CC}_{\nu_e A,i} c$ for nuclei with $A = 100$–200 near the stability line are ∼1–10 times larger than $\lambda_{\nu_e n}$.

When the temperature is above ∼4.5 GK, there is essentially no difference between the cases with and without ν-A reactions. As the temperature becomes lower, and the composition shifts to neutron-rich nuclei, $\lambda^{\rm CC}_{\nu_e A}$ becomes comparable with the expansion rate leading to a faster depletion of neutrons because ν_e absorption on nuclei speeds up the production of heavy elements. The balance between (n,γ) and (γ,n) is broken at ∼3 GK. The rate of (γ,n) decreases drastically, but the rate of (n,γ) changes gradually as neutrons are continuously supplied from the neutrino spallation by both CC and NC ν_e-A reactions. The (n,γ) rate follows $\lambda^{\rm CC}_{\nu_e A}$ and the nucleosynthesis flow is characterized by an equilibrium between (n,γ) and ν_e-A reactions. This produces a rather broad abundance distribution that reaches from the neutron-deficient to the neutron-rich side of beta stability. Since more neutron-rich isotopes are reached, the average β^- rate increases slightly below $T \sim 3$ GK. The average number of emitted neutrons from the CC ν-A reaction is approximately given by the ratio $\lambda_{(n,\gamma)}/\lambda^{\rm CC}_{\nu_e A}$. (The average rate of NC reactions is about 1 order of magnitude lower than $\lambda^{\rm CC}_{\nu_e A}$.) We note that we do not consider heavy lepton neutrinos. They have higher mean energy and possibly larger flux and hence may amplify the total rate to values comparable to $\lambda^{\rm CC}_{\nu_e A}$.

Neutrinos continue to interact with heavy nuclei and increase Y_e as shown in Fig. 2(b). Neutrino spallation on α particles produces ^{3}H and ^{3}He that are converted into ^{12}C by additional α captures. This is achieved by two-body reactions instead of the triple-alpha reaction, and hence they operate until much lower temperatures. After the production of ^{12}C, a sequence of α captures continues, similarly to the αp and rp processes on accreting neutron stars [44]. As a result, Y_α decreases and $Y_{\rm heavy}$ increases. Protons produced from neutrino spallation are barely used

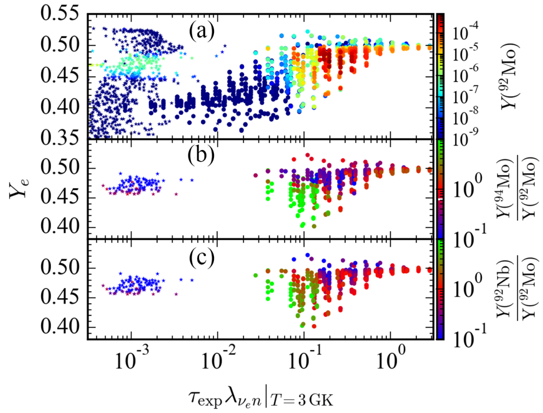

FIG. 3. Scatter plots for the abundance of ^{92}Mo (a), the ratio ^{94}Mo/^{92}Mo (b), and the ratio ^{92}Nb/^{92}Mo (c) with respect to Y_e and neutrino exposure from our parametric survey (circles) and the simulation model sym-n1-a6 (stars) from Ref. [38]. The white line in the color bar in (b) shows the ^{94}Mo/^{92}Mo ratio in solar abundance. (b) and (c) show the abundance ratio only for $Y(^{92}\mathrm{Mo}) > 10^{-7}$.

below ∼4 GK. This together with their production by (n, p) reactions increases Y_p to values $\sim 10^{-3}$. See more details in the Supplemental Material [45].

Survey of conditions.—In addition to the previous three cases, we surveyed a larger parameter space with the following variations: $\delta_\rho = \{0.5, 1, 2, 4, 8\}$ ms, $n_{\nu_e,0} = \{0.25, 0.5, 1, 2\} \times 10^{33}$ cm^{-3}, $R_n = \{0.5, 0.8, 1, 1.2, 1.5, 2, 4\}$, and $\delta_\nu = \{1, 1.5, 2.5, 4, 6\} \times \delta_\rho$, while keeping others the same. We classify the trajectories by the value of Y_e reached at 5 GK and the neutrino exposure. As a measure of the latter, we use the product of the expansion timescale and the rate for ν_e absorption on neutrons, both evaluated at 3 GK. The three panels of Fig. 3 show the abundance of ^{92}Mo, the abundance ratio ^{94}Mo/^{92}Mo, and the ratio ^{92}Nb/^{92}Mo at 1 Myr, respectively. For low values of the neutrino exposure all calculations are concentrated around $Y_e \approx 0.4$ because of our choice of $Y_{e,0}$. High neutrino exposure makes all calculations converge to $Y_e \approx 0.5$. We observe large variations of the abundance yields in the intermediate region. Significant amounts of ^{92}Mo ($\gtrsim 10^{-4}$, corresponding to more than 2.5% of the heavy-element mass when the alpha mass fraction is ≈0.6) are produced when $\tau_{\rm exp}\lambda_{\nu_e n} \gtrsim 0.1$. The ratios ^{94}Mo/^{92}Mo and ^{92}Nb/^{92}Mo are larger for the neutron-rich cases with small neutrino exposure, and are below unity when $Y_e \approx 0.5$.

Figure 3 also shows the nucleosynthesis results for an exemplary neutrino-hydrodynamics simulation of a BNM, namely model sym-n1-a6 of Ref. [38]. In this simulation, neutrino fluxes become negligible by the time nuclei form. Consequently, p nuclei around $A \sim 92$ are produced by the α process operating in a narrow window of $Y_e \sim 0.45$–0.48 while p nuclei heavier than ^{92}Mo are underproduced. However, the conditions in current models are not very far off, and the desired neutrino exposure can be achieved for the same trajectories at earlier times when $T = 10$ GK as shown in the Supplemental Material [45]. The comparison suggests that although purely neutrino-driven winds are not well suited for the νr process, outflows not driven by thermal expansion may be more promising, because their temperature is lower close to the central object with high neutrino fluxes. We speculate that the νr process may operate in magnetically driven ejecta subject to strong neutrino fluxes, which are likely found in polar regions of magnetorotational supernovae [46] and collapsar engines [47], or around magnetized remnants of BNMs [48–50].

Observables.—Assuming that the νr process produces p nuclei in an astrophysical site where also the r process operates and that the yields of both follow solar proportions, we can obtain constraints on the relative contributions of the νr process and the r process to the ejecta. If the whole solar inventory of p and r nuclei is produced on the same site, we expect a ratio of ∼90/1 between the r process and νr process material. We notice that the observation of Sr in the kilonova transient AT2017gfo and the low lanthanide mass fraction inferred from multiband light-curve analyses requires the production of all r-process nuclei [51], assuming solar proportions.

We show in Fig. 4(a) the production factors of p nuclei, i.e., the abundances normalized to the solar value $Y_i/Y_{i,\odot}$ for case I. The gray band, which covers 1 order of magnitude right below the largest abundance, illustrates the isotopes that are expected to be coproduced. The main productions of p nuclei in cases I and II are from ^{78}Kr to ^{102}Pd and from ^{98}Ru to ^{138}La, respectively. Given that case II requires very high neutrino fluxes, we expect that it is more rare than case I. Therefore, we combine 20% from case II with 80% from case I in Fig. 4(b), which yields a pattern that is in good agreement with the solar abundances of the p nuclei from ^{78}Kr to ^{138}La. The νr process does not only produces nuclei commonly associated to the γ process, but also ^{138}La and ^{180}Ta that are often associated with the ν process [22].

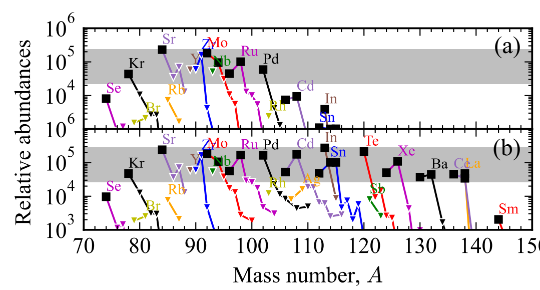

FIG. 4. Relative ratios of p-nuclei (black squares) and other isotopes (colored triangles) over the solar abundance [52] for case I (a) and case I plus 20% of case II (b). Nuclei in the gray bands have a relative abundance within an order of magnitude of the maximum.

Associating the origin of the p nuclei with an r process site, such as BNMs, may have implications for the correlated excesses between p and r nuclei of Mo in primitive meteorites [53]. We can further estimate the time since the last νr process addition to the solar system by considering the short-lived radioactive isotope ^{92}Nb. The νr process results in an abundance ratio between ^{92}Nb and ^{92}Mo that is close to unity, as shown in Fig. 3(c), which is $\sim 10^3$ larger than the ratio $\sim \mathcal{O}(10^{-3})$ found from the ν process in CCSNe [18,22]. Assuming a production ratio close to unity in a simple model of uniform production over the age of the Universe [54,55] and supposing that both ^{92}Mo and ^{92}Nb are predominantly made from the νr process, the ratio in the interstellar medium is $\sim 5 \times 10^{-3}$ after 10 Gyr of evolution. This rough estimate suggests a decay time of ~250 Myr since the last event to match the ESS ratio, which is consistent with the expected time of ~100 Myr since the last r process event [56,57].

Since the νr process depends on the neutrino flux, it could be significantly affected by collective neutrino flavor phenomena [58–63]. In addition, the process depends on the competition between neutrino absorption and neutron captures near the stability line, which calls for further improved measurements of the reaction rates in the laboratory. In this Letter, we have considered moderately neutron-rich ejecta and shown that large neutrino fluxes can drive the composition to the neutron-deficient site of the stability valley producing p nuclei, not only for Mo and Ru but also heavier ones. One can wonder if a reverse process may operate in proton-rich ejecta driving the composition from the neutron-deficient side to the neutron-rich side by $\bar{\nu}_e$-A reactions and producing r nuclei. We expect that this will not be the case as neutron-deficient nuclei still have a neutron excess and hence similar or even larger cross sections for ν_e-A absorption than $\bar{\nu}_e$-A absorption. It remains to be explored if variations of the neutrino flux can produce abundance patterns that resemble those of the s process or i process.

Note added.—A recent study [64] has reported that suitable conditions for the νr-process may exist in winds from rotating highly magnetized proto-neutron stars.

We thank Andreas Bauswein, Karlheinz Langanke, Yong-Zhong Qian, Ninoy Rahman, and Friedrich-Karl Thielemann for fruitful discussions. G. M. P. and Z. X. acknowledge support by the European Research Council (ERC) under the European Union's Horizon 2020 research and innovation programme (ERC Advanced Grant KILONOVA No. 885281). O. J. acknowledges support by the ERC under Grant Agreement No. 759253. O. J., G. M. P., and Z. X. acknowledge support by the Deutsche Forschungsgemeinschaft (DFG, German Research Foundation)—Project-ID 279384907—SFB 1245, and MA 4248/3-1. G. M. P. and O. J. acknowledge support by the State of Hesse within the Cluster Project ELEMENTS. G. M. P. thanks the hospitality of the Instituto de Física Teórica UAM-CSIC, supported by the Severo Ochoa Excellence Program No. CEX2020-001007-S funded by MCIN/AEI, where part of this work was done. A. S. acknowledges funding from the European Union's Framework Programme for Research and Innovation Horizon Europe under Marie Sklodowska-Curie Grant Agreement No. 101065891.

*Corresponding author: z.xiong@gsi.de

[1] M. Arnould and S. Goriely, The p-process of stellar nucleosynthesis: Astrophysics and nuclear physics status, Phys. Rep. **384**, 1 (2003).

[2] M. Pignatari, K. Göbel, R. Reifarth, and C. Travaglio, The production of proton-rich isotopes beyond iron: The γ-process in stars, Int. J. Mod. Phys. E **25**, 1630003 (2016).

[3] C. Fröhlich, G. Martínez-Pinedo, M. Liebendörfer, F. K. Thielemann, E. Bravo, W. R. Hix, K. Langanke, and N. T. Zinner, Neutrino-induced nucleosynthesis of A > 64 nuclei: The νp process, Phys. Rev. Lett. **96**, 142502 (2006).

[4] J. Pruet, R. D. Hoffman, S. E. Woosley, H.-T. Janka, and R. Buras, Nucleosynthesis in early supernova winds II: The role of neutrinos, Astrophys. J. **644**, 1028 (2006).

[5] S. Wanajo, The rp-process in neutrino-driven winds, Astrophys. J. **647**, 1323 (2006).

[6] H. Schatz, A. Aprahamian, J. Görres, M. Wiescher, T. Rauscher, J. Rembges, F.-K. Thielemann, B. Pfeiffer, P. Möller, K.-L. Kratz, H. Herndl, B. A. Brown, and H. Rebel, rp-process nucleosynthesis at extreme temperature and density conditions, Phys. Rep. **294**, 167 (1998).

[7] T. Hayakawa, N. Iwamoto, T. Shizuma, T. Kajino, H. Umeda, and K. Nomoto, Evidence for nucleosynthesis in the supernova γ process: Universal scaling for p nuclei, Phys. Rev. Lett. **93**, 161102 (2004).

[8] M. Kusakabe, N. Iwamoto, and K. Nomoto, Production of the p-process nuclei in the carbon-deflagration model for Type Ia supernovae, Astrophys. J. **726**, 25 (2011).

[9] C. Travaglio, F. K. Röpke, R. Gallino, and W. Hillebrandt, Type Ia supernovae as sites of the p-process: Two-dimensional models coupled to nucleosynthesis, Astrophys. J. **739**, 93 (2011).

[10] S. Wanajo, H. T. Janka, and S. Kubono, Uncertainties in the νp-process: Supernova dynamics versus nuclear physics, Astrophys. J. **729**, 46 (2011).

[11] R. Bollig, N. Yadav, D. Kresse, H.-T. Janka, B. Müller, and A. Heger, Self-consistent 3D supernova models from −7 minutes to +7 s: A 1-bethe explosion of a $\sim 19 m_\odot$ progenitor, Astrophys. J. **915**, 28 (2021).

[12] T. Fischer, G. Guo, A. A. Dzhioev, G. Martínez-Pinedo, M.-R. Wu, A. Lohs, and Y.-Z. Qian, Neutrino signal from proto-neutron star evolution: Effects of opacities from charged-current–neutrino interactions and inverse neutron decay, Phys. Rev. C **101**, 025804 (2020).

[13] R. D. Hoffman, S. E. Woosley, G. M. Fuller, and B. S. Meyer, Production of the light p-process nuclei in neutrino-driven winds, Astrophys. J. **460**, 478 (1996).

[14] S. Wanajo, B. Müller, H.-T. Janka, and A. Heger, Nucleosynthesis in the innermost ejecta of neutrino-driven supernova explosions in two dimensions, Astrophys. J. **852**, 40 (2018).

[15] A. Sieverding, B. Müller, and Y.-Z. Qian, Nucleosynthesis of an 11.8 msun supernova with 3D simulation of the inner ejecta: Overall yields and implications for short-lived radionuclides in the early solar system, Astrophys. J. **904**, 163 (2020).

[16] N. Dauphas, T. Rauscher, B. Marty, and L. Reisberg, Short-lived p-nuclides in the early solar system and implications on the nucleosynthetic role of x-ray binaries, Nucl. Phys. **A719**, C287 (2003).

[17] N. Dauphas and M. Chaussidon, A perspective from extinct radionuclides on a young stellar object: The sun and its accretion disk, Annu. Rev. Earth Planet Sci. **39**, 351 (2011).

[18] T. Hayakawa, K. Nakamura, T. Kajino, S. Chiba, N. Iwamoto, M. K. Cheoun, and G. J. Mathews, Supernova neutrino nucleosynthesis of the radioactive 92Nb observed in primitive meteorites, Astrophys. J. Lett. **779**, 9 (2013).

[19] Y. Hibiya, T. Iizuka, H. Enomoto, and T. Hayakawa, Evidence for enrichment of niobium-92 in the outer protosolar disk, Astrophys. J. Lett. **942**, L15 (2023).

[20] T. Rauscher, N. Dauphas, I. Dillmann, C. Fröhlich, Z. Fülöp, and G. Gyürky, Constraining the astrophysical origin of the p-nuclei through nuclear physics and meteoritic data, Rep. Prog. Phys. **76**, 066201 (2013).

[21] M. Lugaro, M. Pignatari, U. Ott, K. Zuber, C. Travaglio, G. Gyürky, and Z. Fülöp, Origin of the p-process radionuclides ^{92}Nb and ^{146}Sm in the early solar system and inferences on the birth of the Sun, Proc. Natl. Acad. Sci. U.S.A. **113**, 907 (2016).

[22] A. Sieverding, G. Martínez-Pinedo, L. Huther, K. Langanke, and A. Heger, The ν-process in the light of an improved understanding of supernova neutrino spectra, Astrophys. J. **865**, 143 (2018).

[23] A. Sieverding, K. Langanke, G. Martínez-Pinedo, R. Bollig, H.-T. Janka, and A. Heger, The ν-process with fully time-dependent supernova neutrino emission spectra, Astrophys. J. **876**, 151 (2019).

[24] A. Arcones and F.-K. Thielemann, Neutrino-driven wind simulations and nucleosynthesis of heavy elements, J. Phys. G **40**, 013201 (2013).

[25] S. Goriely, A. Bauswein, O. Just, E. Pllumbi, and H. T. Janka, Impact of weak interactions of free nucleons on the r-process in dynamical ejecta from neutron star mergers, Mon. Not. R. Astron. Soc. **452**, 3894 (2015).

[26] D. Martin, A. Perego, W. Kastaun, and A. Arcones, The role of weak interactions in dynamic ejecta from binary neutron star mergers, Classical Quantum Gravity **35**, 034001 (2018).

[27] J. J. Cowan, C. Sneden, J. E. Lawler, A. Aprahamian, M. Wiescher, K. Langanke, G. Martínez-Pinedo, and F. K. Thielemann, Origin of the heaviest elements: The rapid neutron-capture process, Rev. Mod. Phys. **93**, 015002 (2021).

[28] I. Kullmann, S. Goriely, O. Just, R. Ardevol-Pulpillo, A. Bauswein, and H. T. Janka, Dynamical ejecta of neutron star mergers with nucleonic weak processes I: Nucleosynthesis, Mon. Not. R. Astron. Soc. **510**, 2804 (2022).

[29] D. Watson, C. J. Hansen, J. Selsing, A. Koch, D. B. Malesani, A. C. Andersen, J. P. U. Fynbo, A. Arcones, A. Bauswein, S. Covino, A. Grado, K. E. Heintz, L. Hunt, C. Kouveliotou, G. Leloudas, A. J. Levan, P. Mazzali, and E. Pian, Identification of strontium in the merger of two neutron stars, Nature (London) **574**, 497 (2019).

[30] B. S. Meyer, G. C. McLaughlin, and G. M. Fuller, Neutrino capture and r-process nucleosynthesis, Phys. Rev. C **58**, 3696 (1998).

[31] K. Langanke and G. Martínez-Pinedo, Nuclear weak-interaction processes in stars, Rev. Mod. Phys. **75**, 819 (2003).

[32] G. M. Fuller and B. S. Meyer, Neutrino capture and supernova nucleosynthesis, Astrophys. J. **453**, 792 (1995).

[33] G. C. McLaughlin and G. M. Fuller, Evidence for an intense neutrino flux during r-process nucleosynthesis?, Astrophys. J. **464**, L143 (1996).

[34] Y. Z. Qian, W. C. Haxton, K. Langanke, and P. Vogel, Neutrino-induced neutron spallation and supernova r-process nucleosynthesis, Phys. Rev. C **55**, 1532 (1997).

[35] S. E. Woosley and R. D. Hoffman, The alpha-process and the r-process, Astrophys. J. **395**, 202 (1992).

[36] J. Witti, H.-T. Janka, and K. Takahashi, Nucleosynthesis in neutrino-driven winds from protoneutron stars I. The α-process, Astron. Astrophys. **286**, 841 (1994).

[37] C. E. Collins, A. Bauswein, S. A. Sim, V. Vijayan, G. Martínez-Pinedo, O. Just, L. J. Shingles, and M. Kromer, 3D radiative transfer kilonova modelling for binary neutron star merger simulations, Mon. Not. R. Astron. Soc. **521**, 1858 (2023).

[38] O. Just, V. Vijayan, Z. Xiong, A. Bauswein, S. Goriely, J. Guilet, H.-T. Janka, and G. Martínez-Pinedo, End-to-end kilonova models of neutron-star mergers with delayed black-hole formation, Astrophys. J. Lett. **951**, L12 (2023).

[39] J. D. J. Mendoza-Temis, M. R. Wu, K. Langanke, G. Martínez-Pinedo, A. Bauswein, and H. T. Janka, Nuclear robustness of the r process in neutron-star mergers, Phys. Rev. C **92**, 055805 (2015).

[40] M. Reichert, C. Winteler, O. Korobkin, A. Arcones, J. Bliss, M. Eichler, U. Frischknecht, C. Fröhlich, R. Hirschi, M. Jacobi, J. Kuske, G. Martínez-Pinedo, D. Martin, D. Mocelj, T. Rauscher, and F. K. Thielemann, The nuclear reaction network WinNet, Astrophys. J. Suppl. Ser. **268**, 66 (2023).

[41] O. Just, A. Bauswein, R. Ardevol Pulpillo, S. Goriely, and H. T. Janka, Comprehensive nucleosynthesis analysis for ejecta of compact binary mergers, Mon. Not. R. Astron. Soc. **448**, 541 (2015).

[42] S. Goriely, Uncertainties in the solar system r-abundance distribution, Astron. Astrophys. **342**, 881 (1999).

[43] J. Bliss, A. Arcones, and Y.-Z. Qian, Production of Mo and Ru isotopes in neutrino-driven winds: Implications for solar abundances and presolar grains, Astrophys. J. **866**, 105 (2018).

[44] H. Schatz and K. Rehm, X-ray binaries, Nucl. Phys. **A777**, 601 (2006).

[45] See Supplemental Material at http://link.aps.org/supplemental/10.1103/PhysRevLett.132.192701 for more details, which includes Refs. [3,35,36,38,44].

[46] M. Obergaulinger and M. Reichert, Nucleosynthesis in jet-driven and jet-associated supernovae, in *Handbook of Nuclear Physics* (Springer, New York, 2022), pp. 1–38.

[47] D. M. Siegel, J. Barnes, and B. D. Metzger, Collapsars as a major source of r-process elements, Nature (London) **569**, 241 (2019).

[48] J. M. Miller, B. R. Ryan, J. C. Dolence, A. Burrows, C. J. Fontes, C. L. Fryer, O. Korobkin, J. Lippuner, M. R. Mumpower, and R. T. Wollaeger, Full transport model of GW170817-like disk produces a blue kilonova, Phys. Rev. D **100**, 023008 (2019).

[49] M. Shibata, S. Fujibayashi, and Y. Sekiguchi, Long-term evolution of neutron-star merger remnants in general relativistic resistive magnetohydrodynamics with a mean-field dynamo term, Phys. Rev. D **104**, 063026 (2021).

[50] P. Mösta, D. Radice, R. Haas, E. Schnetter, and S. Bernuzzi, A magnetar engine for short GRBs and kilonovae, Astrophys. J. **901**, L37 (2020).

[51] M.-R. Wu, J. Barnes, G. Martínez-Pinedo, and B. D. Metzger, Fingerprints of heavy-element nucleosynthesis in the late-time lightcurves of kilonovae, Phys. Rev. Lett. **122**, 062701 (2019).

[52] M. Asplund, N. Grevesse, A. J. Sauval, and P. Scott, The chemical composition of the sun, Annu. Rev. Astron. Astrophys. **47**, 481 (2009).

[53] T. Stephan, R. Trappitsch, P. Hoppe, A. M. Davis, M. J. Pellin, and O. S. Pardo, Molybdenum isotopes in presolar silicon carbide grains: Details of s-process nucleosynthesis in parent stars and implications for r- and p-processes, Astrophys. J. **877**, 101 (2019).

[54] G. J. Wasserburg, M. Busso, R. Gallino, and K. M. Nollett, Short-lived nuclei in the early solar system: Possible AGB sources, Nucl. Phys. **A777**, 5 (2006).

[55] G. R. Huss, B. S. Meyer, G. Srinivasan, J. N. Goswami, and S. Sahijpal, Stellar sources of the short-lived radionuclides in the early solar system, Geochim. Cosmochim. Acta **73**, 4922 (2009).

[56] M. Lugaro, A. Heger, D. Osrin, S. Goriely, K. Zuber, A. I. Karakas, B. K. Gibson, C. L. Doherty, J. C. Lattanzio, and U. Ott, Stellar origin of the ^{182}Hf cosmochronometer and the presolar history of solar system matter, Science **345**, 650 (2014).

[57] M. Lugaro, U. Ott, and Á. Kereszturi, Radioactive nuclei from cosmochronology to habitability, Prog. Part. Nucl. Phys. **102**, 1 (2018).

[58] H. Duan, A. Friedland, G. C. McLaughlin, and R. Surman, The influence of collective neutrino oscillations on a supernova r process, J. Phys. G Nucl. Part. **38**, 035201 (2011).

[59] Z. Xiong, A. Sieverding, M. Sen, and Y.-Z. Qian, Potential impact of fast flavor oscillations on neutrino-driven winds and their nucleosynthesis, Astrophys. J. **900**, 144 (2020).

[60] M. George, M.-R. Wu, I. Tamborra, R. Ardevol-Pulpillo, and H.-T. Janka, Fast neutrino flavor conversion, ejecta properties, and nucleosynthesis in newly-formed hypermassive remnants of neutron-star mergers, Phys. Rev. D **102**, 103015 (2020).

[61] X. Li and D. M. Siegel, Neutrino fast flavor conversions in neutron-star postmerger accretion disks, Phys. Rev. Lett. **126**, 251101 (2021).

[62] O. Just, S. Abbar, M. R. Wu, I. Tamborra, H. T. Janka, and F. Capozzi, Fast neutrino conversion in hydrodynamic simulations of neutrino-cooled accretion disks, Phys. Rev. D **105**, 083024 (2022).

[63] R. Fernández, S. Richers, N. Mulyk, and S. Fahlman, The fast flavor instability in hypermassive neutron star disk outflows, Phys. Rev. D **106**, 103003 (2022).

[64] T. Prasanna, M. S. Coleman, and T. A. Thompson, Favorable conditions for heavy element nucleosynthesis in rotating proto-magnetar winds, arXiv:2402.06003.